Jamming transition in granular media: A mean-field approximation and numerical simulations

A. Fierro,[1,2] M. Nicodemi,[1,2] M. Tarzia,[1] A. de Candia,[1] and A. Coniglio[1,2]
[1]*Dipartimento di Scienze Fisiche, Università degli Studi di Napoli "Federico II," INFM and INFN, via Cinthia, 80126 Napoli, Italy*
[2]*INFM—Coherentia, Napoli, Italy*

(Received 3 December 2004; revised manuscript received 16 March 2005; published 28 June 2005)

In order to study analytically the nature of the jamming transition in granular material, we have considered a cavity method mean-field theory, in the framework of a statistical mechanics approach, based on Edwards' original idea. For simplicity, we have applied the theory to a lattice model, and a transition with exactly the same nature of the glass transition in mean-field models for usual glass formers is found. The model is also simulated in three dimensions under tap dynamics, and a jamming transition with glassy features is observed. In particular, two-step decays appear in the relaxation functions and dynamic heterogeneities resembling ones usually observed in glassy systems. These results confirm early speculations about the connection between the jamming transition in granular media and the glass transition in usual glass formers, giving moreover a precise interpretation of its nature.

DOI: 10.1103/PhysRevE.71.061305 PACS number(s): 45.70.Cc, 05.50.+q, 64.70.Pf

I. INTRODUCTION

A deep connection between glass transition in molecular glass formers, structural arrest in colloidal systems, and jamming transition in granular media [1–6] has often been stressed in the past few years. In spite of the fact that these systems are very different from one another, varying suitably the control parameters, a slowdown and a subsequent structural arrest in a solidlike disordered state are found in each of them. In [2,6], a possible phase diagram for jamming is suggested, which takes into account the fact that jamming is obtained either raising the volume fraction or lowering the temperature or lowering the applied stress. Colloidal suspensions and molecular glass formers are both thermal systems, and it is commonly accepted that both colloidal glass transition and molecular glass transition are of the same type despite the fact that different control parameters may drive the transition. The case of granular materials is instead very different: They are athermal systems, since the thermal fluctuations are significantly less than the gravitational energy and the system cannot explore the phase space without any external driving. Nevertheless, an exceeding slowing down is observed when a granular material is shaken at low shaking amplitude, or flows under a low shear stress, with strong analogies with the slowing down observed in glass formers. Experimental and numerical studies [4–7] have confirmed this connection, however its precise nature is still unclear [3,6].

In the present paper, in order to study this connection we apply a statistical mechanics approach to granular media. This approach, which has been extensively developed in previous works [8,9], is based on an elaboration of the original ideas suggested by Edwards [10]. The basic assumption is that for a granular system subject to an external drive (e.g., tapping), after having reached stationarity, time averages coincide with suitable ensemble averages over the "mechanically stable" states. We have shown [9] that this assumption works for different lattice models, namely that a generalized Gibbs distribution of the stable states describes with good approximation the stationary state attained by the system under tapping dynamics. Here each tap consists in raising the bath temperature to a finite value (called tap amplitude) and, after a lapse of time (called tap duration), quenching the bath temperature back to zero. By cyclically repeating the process, the system explores the space of the mechanically stable states.

We thus consider one of the above lattice models for which the statistical mechanics approach works. The model is made up of hard spheres under gravity. Then we apply standard statistical mechanics methods in order to investigate analytically the existence and the nature of a possible jamming transition. More precisely, we consider the Bethe-Peierls approximation using the cavity method [11,12]: By changing the control parameter, a phase transition from a fluid to a crystal is found, and, when crystallization is avoided, a glassy phase appears. The nature of this glassy phase is analogous to that found in mean-field models for glass formers [12–14]: In particular, we observe a dynamical transition, where an exponentially high number of metastable states appears, and at a lower temperature a thermodynamic discontinuous phase transition to a glassy state. A brief account of these calculations was given in a previous Letter [15]. We also studied [15] the model in 3D by means of numerical simulations, and we found that the model under taps has a transition from a fluid to a crystal, in very good agreement with the mean-field approximation. However, the numerical simulation was not suitable to study the glass transition since the model showed a strong tendency towards crystallization.

For this reason, we study here a variant of the model [13] which has the virtue of avoiding crystallization. We find that the system under gravity evolved by Monte Carlo taps presents features characteristic of real granular media [16,17], and at low tap amplitudes a strong slowing down in the dynamics with properties recalling those of usual glass formers. In particular, we observe a dynamical nonlinear susceptibility with a maximum at increasing time: This behavior, typical of glass formers, is usually interpreted as the sign of dynamic heterogeneities in the system.

In conclusion, the results confirm early speculations about the deep connection between the jamming transition in granular media and the glass transition in usual glass formers, giving moreover a precise interpretation to its nature.

In Sec. II, the mean-field phase diagram is discussed. The details of calculations are presented in Appendixes A and B. In particular, in Appendix B the self-consistency equations obtained using the cavity method are shown. In Sec. III, the 3D model is presented and the numerical results are shown.

II. MEAN-FIELD SOLUTION IN THE BETHE-PEIERLS APPROXIMATION

The model is a monodisperse hard-sphere system (with diameter $\sqrt{2}a_0$) under gravity. The Hamiltonian is given by

$$\mathcal{H} = \mathcal{H}_{\mathrm{HC}} + mg\sum_i n_i z_i, \tag{1}$$

where z_i is the height of site i, g is the gravity acceleration, m is the grain mass, $n_i \in \{0,1\}$ is the occupancy variable (absence or presence of a grain on site i), and $\mathcal{H}_{\mathrm{HC}}(\{n_i\})$ is the hard-core term preventing two nearest-neighbor sites from being simultaneously occupied.

We have shown in previous papers [9] that the model, Eq. (1), under taps can be described with good approximation by a generalized Gibbs distribution of the "mechanically stable" states (i.e., the states where the system is found at rest). In particular, we have studied the model, Eq. (1), on a cubic lattice of spacing a_0. In our Monte Carlo simulations, a sequence of taps is applied to the system: Each tap consists in raising the bath temperature, T_{bath}, to a finite value, and after a given time, quenching T_{bath} back to zero. We wait for the system to stop, and the measures are done in these mechanically stable states. We have found that the weight of a given state, $\{n_i\}$, is given with good approximation by

$$\mathrm{e}^{-\beta H(\{n_i\})}\Pi(\{n_i\}), \tag{2}$$

where $K_B T_{conf} = \beta^{-1}$ is a thermodynamic parameter, called "configurational temperature," characterizing the distribution. The operator $\Pi(\{n_i\})$ selects mechanically stable states: $\Pi(\{n_i\})=1$ if $\{n_i\}$ is "stable" and $\Pi(\{n_i\})=0$ otherwise. The system partition function is thus the following [9]:

$$\mathcal{Z} = \sum_{\{n_i\}} \mathrm{e}^{-\beta H(\{n_i\})}\Pi(\{n_i\}), \tag{3}$$

where the sum runs over all microstates, $\{n_i\}$.

In the present section, we show the phase diagram of the model, Eq. (1), obtained using a mean-field theory in the Bethe-Peierls approximation (see [11,12] and references therein), based on a random graph (plotted in Fig. 1) which takes into account that the gravity breaks up the symmetry along the z axis. This lattice is made up of H horizontal layers (i.e., $z \in \{1,\ldots,H\}$). Each layer is a random graph of connectivity, $k-1=3$. Each site in layer z is also connected to its homologous site in $z-1$ and $z+1$ (the total connectivity is thus $k+1$). Locally, the graph has a treelike structure but there are loops whose length is of order $\ln N$, insuring geometric frustration. In the thermodynamic limit, only very long loops are present. We adopt a simple definition of "mechanical stability:" a grain is "stable" if it has a grain underneath. For a given grain configuration $\{n_i\}$, the operator $\Pi(\{n_i\})$ has a simple expression: $\Pi(\{n_i\}) = \lim_{K\to\infty} \exp\{-K\mathcal{H}_{Edw}\}$, where $\mathcal{H}_{Edw} = \Sigma_i \delta_{n_i(z),1}\delta_{n_i(z-1),0}\delta_{n_i(z-2),0}$ [for clarity, we have shown the z dependence in $n_i(z)$]. The details of the calculations are given in Appendixes A and B (see also Refs. [15,18], where this mean-field theory was first introduced).

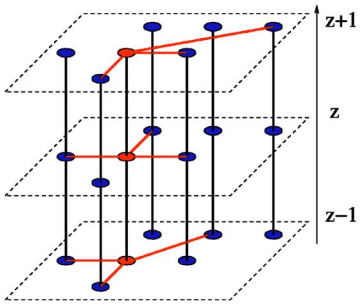

FIG. 1. (Color online) In the mean-field approximation, the grains are located on a Bethe lattice, sketched in the figure, where each horizontal layer is a random graph of connectivity $k-1=3$. Homologous sites on neighboring layers are also linked and the overall connectivity, $c \equiv k+1=5$ (z is in units of a_0).

We solve the recurrence equations found in the Bethe-Peierls approximation in three cases: (1) A fluidlike homogeneous phase; (2) a crystallinelike phase characterized by the breakdown of the horizontal translational invariance; and (3) a glassy phase described by a one-step replica symmetry breaking (1RSB). The details of the calculations are shown in the Appendixes.

The control parameters are the configurational temperature, T_{conf}, and the number of grains per unit surface, $N_s = \Sigma_z \sigma(z)$, $\sigma(z)$ being the density profile. In Fig. 2, the bulk density at equilibrium, $\Phi \equiv N_s/(2\langle z\rangle - 1)$ [19] (where $\langle z\rangle$ is the average height), is plotted as a function of the configu-

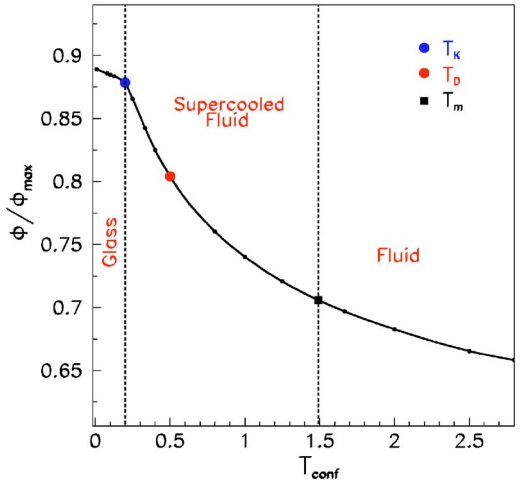

FIG. 2. (Color online) The density, $\Phi \equiv N_s/(2\langle z\rangle - 1)$, for $N_s = 0.6$ as a function of T_{conf} (Φ is in units of a_0^{-3} and T_{conf} in units of mga_0/K_B). Φ_{max} is the maximum density reached by the system in the crystal phase.

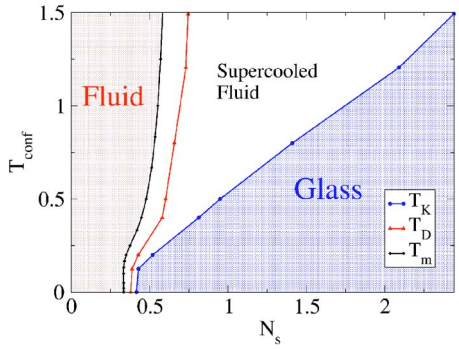

FIG. 3. (Color online) The system mean-field phase diagram is plotted in the plane of its two control parameters (T_{conf}, N_s) (T_{conf} is in units of mga_0/K_B and N_s in units of a_0^{-2}).

rational temperature, T_{conf}, for a given value of N_s. We found that at high T_{conf}, a homogeneous solution corresponding to the fluidlike phase is found. By lowering T_{conf} at T_m, a phase transition to a crystal phase (an antiferromagnetic solution with a breakdown of the translation invariance) occurs. The fluid phase still exists below T_m as a metastable phase corresponding to a supercooled fluid when crystallization is avoided. Finally, a 1RSB solution (found with the cavity method [11]), characterized by the presence of a large number of local minima in the free energy [11,20], appears at T_D, and becomes stable at a lower point T_K, where a thermodynamic transition from the supercooled fluid to a 1RSB glassy phase takes place. The temperature T_D, which is interpreted in mean field as the location of a dynamical transition where the relaxation time diverges, in real systems might instead correspond to a crossover in the dynamics (see [12,14,21] and references therein). $\Phi(T_{conf})$ has a shape very similar to that observed in the "reversible regime" of tap experiments [16,23]. The location of the glass transition, T_K, corresponds to a cusp in the function $\Phi(T_{conf})$. The dynamical crossover point T_D might correspond to the position of a characteristic shaking amplitude Γ^* found in experiments and simulations where the "irreversible" and "reversible" regimes approximately meet.

In Fig. 3, the phase diagram obtained by varying N_s is shown. The dashed vertical line in the figure corresponds to the value of N_s chosen in Fig. 2.

The model, Eq. (1), simulated in 3D by means of Monte Carlo tap dynamics [15] presents a transition from a fluid to a crystal as predicted by the mean-field approximation, density profiles in good agreement with the mean-field ones, and in the fluid phase a large increase of the relaxation time as a function of the inverse tap amplitude. In the following section, we study a more complex model for hard spheres, where an internal degree of freedom allows us to avoid crystallization [13].

III. HARD SPHERES WITH AN INTERNAL DEGREE OF FREEDOM

The Hamiltonian of the model is

$$\mathcal{H} = \sum_{\langle ij \rangle} n_i n_j \phi_{ij}(\sigma_i, \sigma_j) + mg \sum_i n_i z_i, \tag{4}$$

where z_i is the height of site i, g is the gravity acceleration, m the grain mass, $n_i \in \{0,1\}$ is the occupancy variable (absence

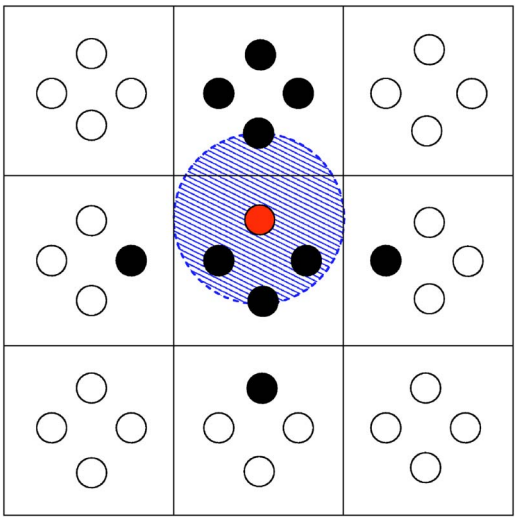

FIG. 4. The model in two dimensions: the space is partitioned in square cells, and each cell can be occupied by at most one particle in any one of the four shown positions (little circles). A particle in any given position (large shaded circle) excludes the presence of particles in any of the black colored positions.

or presence of a grain on site i), $\sigma_i \in \{1, \ldots, q\}$ represents the internal degree of freedom (which we call spin), and $\phi_{ij}(\sigma_i, \sigma_j)$ is the interaction energy between spins. Different values of the spin correspond to different positions of the particle inside the cell. It is reasonable that a few number of internal states might be enough to catch the main features of real systems.

As in Ref. [13], we study a simple realization of the model described by Eq. (4). Interpreting the spin as a position of the particle in the cell, our choice can be easily visualized in 2D, as shown in Fig. 4. We partition the space in square cells, and subdivide each cell into four internal positions (namely $q=4$). When a cell is occupied by a particle in any given position, a hard-core repulsion excludes the presence of particles in some of the internal states of the neighboring cells [namely, the interaction $\phi_{ij}(\sigma_i, \sigma_j)$ is chosen zero if the positions σ_i and σ_j are "compatible" and infinite otherwise]. This choice can be interpreted as a coarse-grained version of a hard-sphere system in the continuum. In 3D we subdivide the space into cubic cells of linear size a_0, and we consider six internal positions instead of four.

In the Monte Carlo simulations, $N=433$ grains are confined in a 3D box of linear size $L=12$ (i.e., $N_s=3$), between hard walls in the vertical direction and with periodic boundary conditions in the horizontal directions. We perform a standard METROPOLIS algorithm on the system. The particles, initially prepared in a random configuration, are subject to taps, each one followed by a relaxation process. During a tap, for a time τ_0 (called tap duration), the temperature is set to the value T_Γ (called tap amplitude), so that particles have a finite probability, p_{up}, to move upwards [22]. During the relaxation the temperature is set to zero, so that particles can only reduce the energy, and therefore can move only downwards. The relaxation stops when the system has reached a blocked state, where no grain can move downwards. Our measurements are performed at this stage when the shake is

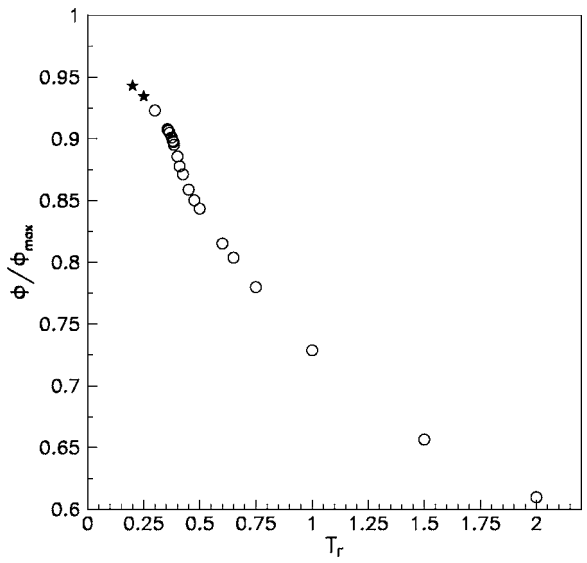

FIG. 5. The bulk density, $\Phi \equiv N/L^2(2\langle z\rangle - 1)$, is plotted as a function of T_Γ (T_Γ is in units of mga_0/K_B and Φ in units of a_0^{-3}) for $\tau_0 = 10$ MC steps/particle. The empty circles correspond to stationary states and the black stars to out of stationarity ones. Φ_{max} is the maximum density reached by the system in the crystal phase, $\Phi_{max} = 6/7a_0^{-3}$.

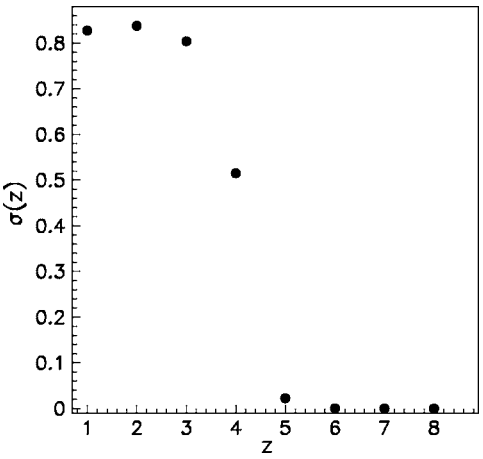

FIG. 6. The density profile, $\sigma(z)$, as function of the height, z, for $T_\Gamma = 0.20\ mga_0/K_B$ and $\tau_0 = 10$ MC steps/particle [z is in units of a_0 and $\sigma(z)$ in units of a_0^{-3}].

off and the system is at rest. The time, t, is the number of taps applied to the system.

In the following, the tap duration is fixed, $\tau_0 = 10$ MC steps/particle and different tap amplitudes, T_Γ, are considered. For each temperature, the quantities of interest are averaged over 16–32 different realizations of the system, and the errors are calculated as the fluctuations over this statistical ensemble. In the following, where the error bars are not plotted, the errors are smaller than the symbol size. In Fig. 5, the bulk density, $\Phi \equiv N/L^2(2\langle z\rangle - 1)$, is plotted as a function of T_Γ: $\Phi(T_\Gamma)$ has a shape resembling that found in the "reversible regime" of tap experiments [16,23], and moreover very similar to that obtained in the mean-field calculations and shown in Fig. 2. At low shaking amplitudes (corresponding to high bulk densities), a strong growth of the equilibration time (i.e., the time necessary to reach stationarity) is observed, and for the lowest values considered here (the black stars in Fig. 5) the system remains out of stationarity. In this region, the density profile, $\sigma(z) \equiv 1/L^2 \Sigma_i n_i(z)$ (where the sum Σ_i is done over the sites i in the layer $z = 1, \ldots, L$ [24]), is almost constant until a given layer and sharply decays to zero (see Fig. 6), as found in real granular media [17]. In conclusion, the system studied here presents a jamming transition at low tap amplitudes as found in real granular media.

In order to test the predictions of the mean-field calculations, in the following we measure quantities usually important in the study of glass transition: the relaxation functions, the relaxation time, and the dynamical susceptibility, connected to the presence a dynamical correlation length.

In particular, we calculate the two-time autocorrelation functions,

$$C(t,t_w) = \frac{1}{N}\sum_i \overline{n_i(t)n_i(t_w)\vec{\sigma}_i(t)\cdot\vec{\sigma}_i(t_w)}, \tag{5}$$

where $\vec{\sigma}_i$ are unit length vectors, pointing in one of the six coordinate directions, representing the position of the particles inside the cell; the average $\overline{(\cdots)}$ is done over 16–32 different realizations of the model obtained varying the random number generator in the simulations, and the errors are calculated as the fluctuations over this statistical ensemble. For values of t_w long enough, the system reaches a stationary state, where the time translation invariance is recovered, i.e., $C(t,t_w) = C(t - t_w)$. In this time region, by averaging $C(t',t_w)$ over t' and t_w such that $t = t' - t_w$ is fixed, we calculate the "equilibrium" autocorrelation functions

$$\langle q(t)\rangle = \langle C(t' - t_w)\rangle \tag{6}$$

and the dynamical nonlinear susceptibility

$$\chi(t) = \langle q(t)^2\rangle - \langle q(t)\rangle^2. \tag{7}$$

As shown in Fig. 7, at low values of the tap amplitudes, T_Γ, two-step decays appear, well fitted in the intermediate time region, by the β correlator predicted by the mode coupling theory for supercooled liquids [25,26] (the continuous curve in Fig. 7), and at long time by stretched exponentials (the dashed curve in figure). The relaxation time, τ, is defined as $\langle q(\tau)\rangle \sim 0.1$ [27].

In Fig. 8, the relaxation time, τ, is plotted as a function of the density, Φ. As found in many glass-forming liquids, $\tau(\Phi)$ is well fitted by a Vogel-Fulcher for the entire range, even if we can identify a first region where $\tau(\Phi)$ is fitted with good approximation by a power law. The power-law divergence can be interpreted as a mean-field behavior, followed by a hopping regime. Note that the model, Eq. (4), studied in the absence of gravity by means of the usual Monte Carlo METROPOLIS [13], exhibits a divergence of the relaxation time as a power law, and no crossover to a hopping regime is observed. We suggest that in the present case, the tap dynamics favors the equilibration via hopping precesses.

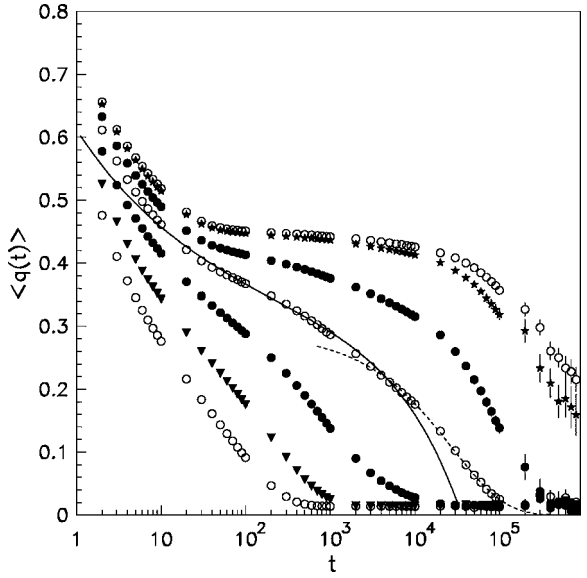

FIG. 7. The "equilibrium" autocorrelation function, $\langle q(t)\rangle$, plotted as function of t (t is in units of tap), for tap amplitudes T_Γ =0.60 0.50, 0.425, 0.40, 0.385, 0.365, and 0.36 mga_0/K_B (from bottom to top). The continuous line in figure is the β correlator of the mode coupling theory with exponent parameters a=0.30 and b=0.52. The dashed line is a stretched exponential $\propto\exp[-(t/\tau_1)^\beta]$ with β=0.70.

In Fig. 9, the relaxation time, τ, is plotted as a function of the tap amplitude, T_Γ: A crossover from a power law to a different regime is again observed around a tap amplitude T_D, corresponding to the value of the density, $\Phi(T_D)\simeq\Phi_D$, where a similar crossover has been found in Fig. 8. However, we cannot exclude that such a crossover is due to a finite-size effect and only the power-law divergence survives in the thermodynamic limit.

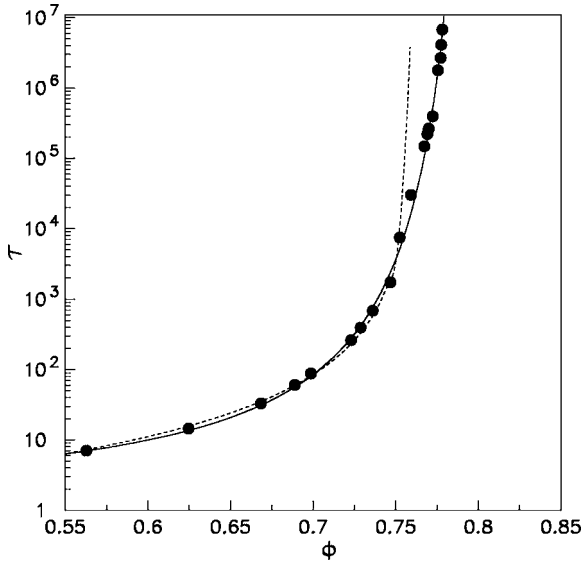

FIG. 8. The relaxation time, τ, as function of the bulk density, Φ (τ is in units of tap and Φ is in units of a_0^{-3}). The continuous line is a Vogel-Fulcher, $e^{A/(\Phi_c-\Phi)}$, with Φ_c=0.81±0.01 and A=0.49±0.10. The dashed line is a power law, $(\Phi_D-\Phi)^{-\gamma_1}$, with Φ_D=0.76±0.01 and γ_1=2.04±0.10.

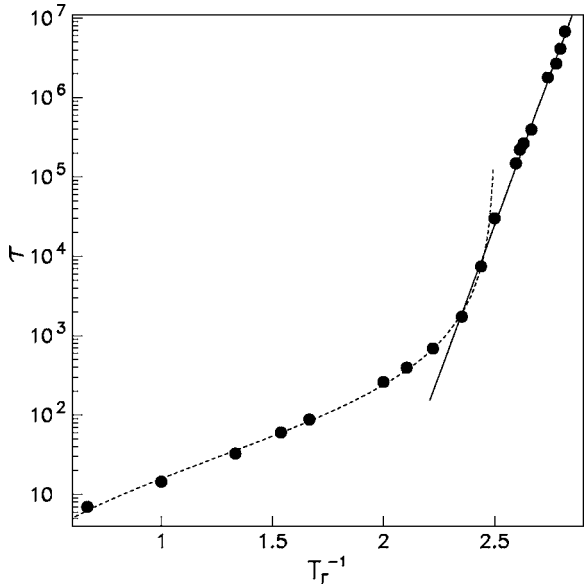

FIG. 9. The relaxation time, τ, as a function of the tap amplitude inverse, T_Γ^{-1} (τ is in units of tap and T_Γ in units of mga_0/K_B). The dashed line is a power law, $(T_\Gamma-T_D)^{-\gamma_2}$, with T_D=0.40±0.01 and γ_2=1.52±0.10. The continuous line is an Arrhenius fit, e^{A/T_Γ}, with A=17.4±0.5 (the data in this region are also well fitted by both a super-Arrhenius and Vogel-Fulcher laws).

The divergence of the relaxation time at vanishing tap amplitude is consistent with the experimental data of Philippe and Bideau [16] and D'Anna *et al.* [4]. Their findings are in fact consistent with an Arrhenius behavior as a function of the experimental tap amplitude intensity. However, a direct comparison with our data is not possible since we do not know the relation between the experimental tap amplitude and the tap amplitude in our simulations. A more direct comparison would be possible if the experimental data were plotted as a function of the bulk density, as we did in Fig. 8.

The dynamical nonlinear susceptibility, $\chi(t)$, plotted in Fig. 10 at different T_Γ, exhibits a maximum at a time, $t^*(T_\Gamma)$, proportional to the relaxation time, $\tau(T_\Gamma)$. A similar behavior was also found in a granular system in Ref. [28]. The presence of a maximum in the dynamical nonlinear susceptibility is typical of glassy systems [29,30]. In particular the value of the maximum, $\chi(t^*)$, diverges in the p-spin model [29] as the dynamical transition is approached from above, signaling the presence of a diverging dynamical correlation length. In the present case, the value of the maximum increases as T_Γ decreases (except at very low T_Γ where the maximum seems to decrease [31]). The growth of $\chi(t^*)$ in our model suggests the presence of a growing dynamical length also in granular media.

IV. CONCLUSIONS

In conclusion, using standard methods of statistical mechanics, we have investigated the jamming transition in a model for granular media. We have shown a deep connection between the jamming transition in granular media and the glass transition in usual glass formers. As in usual glass

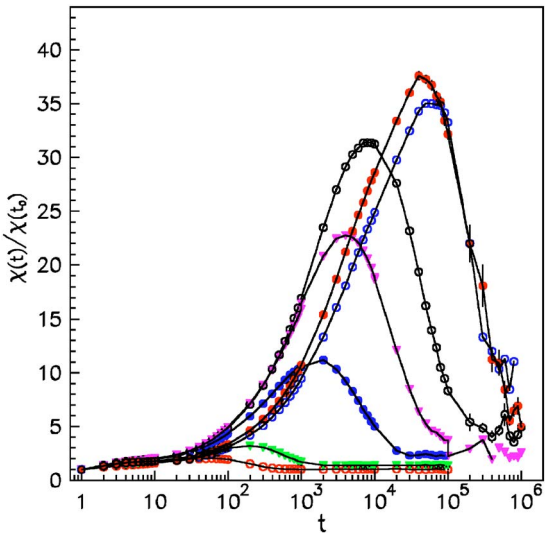

FIG. 10. The dynamical nonlinear susceptibility, $\chi(t)$ [normalized by $\chi(t_0)$, the value at $t_0=1$ tap] as a function of t (t is in units of tap), for tap amplitudes $T_\Gamma=0.60$, 0.50, 0.425, 0.41, 0.40, 0.385, and 0.3825 mga_0/K_B (from left to right).

formers, the mean-field calculations obtained using a statistical mechanics approach to granular media predict a dynamical transition at a finite temperature, T_D, and, at a lower temperature, T_K, a thermodynamics discontinuous phase transition to a glass phase. In finite dimensions (1) the dynamical transition becomes only a dynamical crossover as also found in usual glass formers [12,14,21] (here the relaxation time, τ, as a function of both the density and the tap amplitude, presents a crossover from a power law to a different regime); and (2) the thermodynamics transition temperature, T_K, seems to go to zero (the relaxation time, τ, seems to diverge only at $T_\Gamma \simeq 0$, even if a very low value of the transition temperature is consistent with the data).

ACKNOWLEDGMENTS

We would like to thank M. Pica Ciamarra for many interesting discussions and suggestions. Work supported by EU Network No. MRTN-CT-2003-504712, MIUR-PRIN 2002, MIUR-FIRB 2001, and CRdC-AMRA, INFM-PCI.

APPENDIX A: MEAN-FIELD SOLUTION

We consider the Hamiltonian, Eq. (1), plus a chemical potential term which controls the overall density. Hard-core repulsion prevents two connected sites from being occupied at the same time. We adopt a simple definition of "mechanical stability": a grain is "stable" if it has a grain underneath. For a given grain configuration $\{n_i\}$, the operator $\Pi(\{n_i\})$ has a simple expression: $\Pi(\{n_i\})=\lim_{K\to\infty}\exp\{-K\mathcal{H}_{Edw}\}$, where $\mathcal{H}_{Edw}=\Sigma_i\delta_{n_i(z),1}\delta_{n_i(z-1),0}\delta_{n_i(z-2),0}$ [for clarity, we have shown the z dependence in $n_i(z)$].

The random graph, Fig. 1, keeps into account that the gravity breaks up the symmetry along the z axis. This lattice is made up of H horizontal layers [32] occupied by hard spheres (two numbers identify a site of the lattice: the height

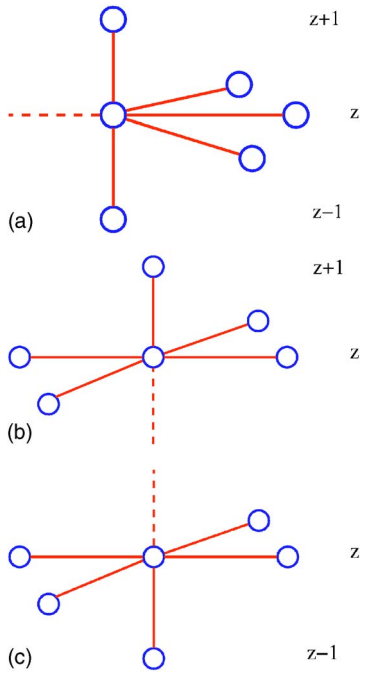

FIG. 11. Three kinds of branches exist here: (a) "side" branch: the root site is connected to $k-2$ neighbors on its layer, one in the upper and one in the lower layer; (b) "up" branch: the root site is connected to $k-1$ neighbors on its layer and one in the upper layer; (c) "down" branch: the root site is connected to $k-1$ neighbors on its layer, one in the lower layer.

of the layer, $z\in\{1,\ldots,H\}$, and the position in the layer, i). Each layer is a random graph of connectivity, $k-1=3$. Each site in a layer at height z is also connected to its homologous site in $z-1$ and $z+1$ (the total connectivity is thus $k+1$). The local treelike structure of the lattice allows us to write down iterative equations in the manner of Bethe, where the partition function of each site is written in terms of the partition functions of the neighbor sites. We have to introduce the concept of "branch": a branch is a graph where a root site, i, has only k neighbors. In the present case, three kinds of branches exist (see Fig. 11): an "up" ("down") branch where the root site has $k-1$ neighbors on its same layer and one in the upper (lower) layer, and a "side" branch where the root has $k-2$ neighbors on its layer, one in the upper and one in the lower layer.

Define $Z_{0,s}^{(i,z)}$ and $Z_{1,s}^{(i,z)}$, the partition functions of a "side" branch with root site i at height z restricted, respectively, to configurations in which the site i is empty or filled by a particle. $Z_{1,u}^{(i,z)}$ and $Z_{0,u}^{(i,z)}$ ($\bar{Z}_{0,u}^{(i,z)}$) are the partition functions of the "up" branch restricted, respectively, to configurations in which the site i is filled by a particle, or empty with the upper site filled (empty). Finally $Z_{1,d}^{(i,z)}$ and $Z_{0,d}^{(i,z)}$ ($\bar{Z}_{0,d}^{(i,z)}$) are the partition functions of the "down" branch restricted, respectively, to configurations in which the site i is filled by a particle, or empty with the lower site empty (filled).

The partition function of the branch ending in site i can be recursively written in terms of the partition functions of the neighbor sites. Summing over all the possible configurations of the neighbor sites, we obtained that the partition function

of a "side" branch with root site i at height z is

$$Z_{0,s}^{(i,z)} = \left[\prod_{j=1}^{k-2}(Z_{0,s}^{(j,z)} + Z_{1,s}^{(j,z)})\right] \times \{Z_{1,u}^{(i,z+1)}[Z_{1,d}^{(i,z-1)} + e^{-K}(\bar{Z}_{0,d}^{(i,z-1)} + Z_{0,d}^{(i,z-1)})] + (\bar{Z}_{0,u}^{(i,z+1)} + e^{-K}Z_{0,u}^{(i,z+1)}) \times (Z_{1,d}^{(i,z-1)} + \bar{Z}_{0,d}^{(i,z-1)} + Z_{0,d}^{(i,z-1)})\},$$

$$Z_{1,s}^{(i,z)} = e^{\beta(\mu - mgz)}\left(\prod_{j=1}^{k-2} Z_{0,s}^{(j,z)}\right)(\bar{Z}_{0,d}^{(i,z-1)} + e^{-K}Z_{0,d}^{(i,z-1)}) \times (\bar{Z}_{0,u}^{(i,z+1)} + Z_{0,u}^{(i,z+1)}). \quad \text{(A1)}$$

In the same way, we can write the recursion relations for the "up" branch,

$$Z_{0,u}^{(i,z)} = \left[\prod_{j=1}^{k-1}(Z_{0,s}^{(j,z)} + Z_{1,s}^{(j,z)})\right] Z_{1,u}^{(i,z+1)},$$

$$\bar{Z}_{0,u}^{(i,z)} = \left[\prod_{j=1}^{k-1}(Z_{0,s}^{(j,z)} + Z_{1,s}^{(j,z)})\right] \bar{Z}_{0,u}^{(i,z+1)},$$

$$Z_{1,u}^{(i,z)} = e^{\beta(\mu - mgz)}\left(\prod_{j=1}^{k-1} Z_{0,s}^{(j,z)}\right)(\bar{Z}_{0,u}^{(i,z+1)} + Z_{0,u}^{(i,z+1)}). \quad \text{(A2)}$$

Finally, for the "down" branch, we have

$$Z_{0,d}^{(i,z)} = \left[\prod_{j=1}^{k-1}(Z_{0,s}^{(j,z)} + Z_{1,s}^{(j,z)})\right](Z_{0,d}^{(i,z-1)} + \bar{Z}_{0,d}^{(i,z-1)}),$$

$$\bar{Z}_{0,d}^{(i,z)} = \left[\prod_{j=1}^{k-1}(Z_{0,s}^{(j,z)} + Z_{1,s}^{(j,z)})\right] Z_{1,d}^{(i,z-1)},$$

$$Z_{1,d}^{(i,z)} = e^{\beta(\mu - mgz)}\left(\prod_{j=1}^{k-1} Z_{0,s}^{(j,z)}\right) \times (\bar{Z}_{0,d}^{(i,z-1)} + e^{-K}Z_{0,d}^{(i,z-1)}). \quad \text{(A3)}$$

In the following, we consider the limit $K \to \infty$ in order to take into account the constraint on the mechanical stability. It is convenient to introduce five local "cavity" fields on each site: $h_s^{(i,z)}$, $h_u^{(i,z)}$, $g_u^{(i,z)}$, $h_d^{(i,z)}$, and $g_d^{(i,z)}$, defined by the following relations: $e^{\beta h_s^{(i,z)}} = Z_{1,s}^{(i,z)}/Z_{0,s}^{(i,z)}$, $e^{\beta h_u^{(i,z)}} = Z_{1,u}^{(i,z)}/\bar{Z}_{0,u}^{(i,z)}$, $e^{\beta g_u^{(i,z)}} = Z_{0,u}^{(i,z)}/\bar{Z}_{0,u}^{(i,z)}$, $e^{\beta h_d^{(i,z)}} = Z_{1,d}^{(i,z)}/\bar{Z}_{0,d}^{(i,z)}$, and $e^{\beta g_d^{(i,z)}} = Z_{0,d}^{(i,z)}/\bar{Z}_{0,u}^{(i,z)}$. In these new variables, the recursion relations are more easily written,

$$e^{\beta h_s^{(i,z)}} = e^{\beta(\mu - mgz)}\left[\prod_{j=1}^{k-2}(1 + e^{\beta h_s^{(j,z)}})^{-1}\right](1 + e^{\beta g_u^{(i,z+1)}}) \times [1 + e^{\beta h_d^{(i,z-1)}} + e^{\beta g_d^{(i,z-1)}} + e^{\beta h_d^{(i,z-1)} + \beta h_u^{(i,z+1)}}]^{-1},$$

$$e^{\beta h_u^{(i,z)}} = e^{\beta(\mu - mgz)}(1 + e^{\beta g_u^{(i,z+1)}})\prod_{j=1}^{k-1}(1 + e^{\beta h_s^{(j,z)}})^{-1},$$

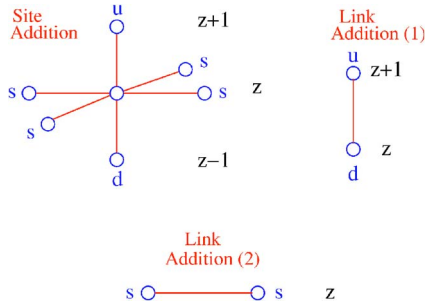

FIG. 12. Site addition: a new central site at height z is connected to $k-1$ side branches (s) with the root sites in the same layer, to one up (u) branch with the root site in the higher layer and to one down (d) branch with the root site in the lower layer. Link addition (1): a link between a down branch with the root site at height z and an up branch with the root site in the higher layer is added. Link addition (2): a link between two side branches with the root site in the same layer is added.

$$e^{\beta g_u^{(i,z)}} = e^{\beta h_u^{(i,z+1)}},$$

$$e^{\beta h_d^{(i,z)}} = e^{\beta(\mu - mgz)}e^{-\beta h_d^{(i,z-1)}}\prod_{j=1}^{k-1}(1 + e^{\beta h_s^{(j,z)}})^{-1},$$

$$e^{\beta g_d^{(i,z)}} = (1 + e^{\beta g_d^{(i,z-1)}})e^{-\beta h_d^{(i,z-1)}}. \quad \text{(A4)}$$

Note that in the case $k=1$, the problem reduces to a simple one-dimensional chain: In this case, the recursive method is equivalent to the transfer-matrix method and gives the exact solution.

From the iterative solution of Eqs. (A4), it is possible to compute the system free energy. Generalizing the procedure followed in [11], we calculate the free-energy density, F, in the thermodynamic limit from the variation of the free energy going from a random graph with H layers and N sites on each layer to one with H layers and $N+2$ sites on each layer. In order to do that, we define the following intermediate object: a random graph with H layers and N sites in each plane such that $2(k+1)$ sites on each plane are connected only to k neighbors instead of $k+1$. In particular, on each layer two sites are not connected to sites on the higher layer ("down" branches), two sites are not connected to sites on the lower layer ("up" branches), and the other $2(k-1)$ are connected only with $k-2$ sites in the plane instead of $k-1$ ("side" branches). From this intermediate object, a random graph with H layers and $N+2$ sites on each layer (all connected to $k+1$ sites) can be obtained adding two new sites to each plane and connecting each of the new sites with $k-1$ side branches on their respective planes, one up branch in the upper layer and one down branch in the lower layer (see Fig. 12). This operation is called "site addition." A random graph with H layers and N sites on each layer (all connected to $k+1$ sites) is instead obtained from the intermediate object adding for each layer two links between the up branches at height z and the down branches at height $z-1$, and $(k-1)$

links between the sides branches on each layer (see Fig. 12). This operation, which allows us to saturate all the missing links, is called "link addition."

Therefore, the variation of the free energy when going from NH to $(N+2)H$ sites (i.e., a random graph with two sites more on each layer) is related to the free-energy shifts (see Fig. 12) for a site addition ($\Delta F^{(z)}_{site}$) and for two different kinds of link addition ($\Delta F^{(z)}_{link,1}$ and $\Delta F^{(z)}_{link,2}$),

$$F_{N+2} - F_N = 2\sum_{z=1}^{H} \Delta F^{(z)}_{site} - (k-1)\sum_{z=1}^{H} \Delta F^{(z)}_{link,2} - 2\sum_{z=1}^{H-1} \Delta F^{(z)}_{link,1},$$

where $F_{N+2}-F_N$ is obtained as $(F_{N+2}-F_0)-(F_N-F_0)$, and F_0 is the free energy of the intermediate object described above. We assume that in the thermodynamic limit, the free energy is linear in N. The free-energy density is then

$$F = \sum_{z=1}^{H} \Delta F^{(z)}_{site} - \frac{(k-1)}{2}\sum_{z=1}^{H} \Delta F^{(z)}_{link,2} - \sum_{z=1}^{H-1} \Delta F^{(z)}_{link,1}. \quad \text{(A5)}$$

In terms of the local fields, the free-energy shifts due to the addition of a site i at height z read

$$e^{-\beta\Delta F^{(i,z)}_{site}} = \left[\prod_{j=1}^{k-1}(1+e^{\beta h_s^{(i,z)}})\right](1+e^{\beta h_d^{(i,z-1)}} + e^{\beta g_d^{(i,z-1)}} + e^{\beta h_d^{(i,z-1)}} e^{\beta h_u^{(i,z+1)}}) + e^{\beta(\mu-mgz)}(1+e^{\beta g_u^{(i,z+1)}}). \quad \text{(A6)}$$

The free-energy shift due to a link addition between a down branch with the root site at height z and an up branch with the root site at height $z+1$ is given by

$$e^{-\beta\Delta F^{(i,z|z+1)}_{link,1}} = 1 + e^{\beta g_d^{(i,z)}} + e^{\beta h_u^{(i,z+1)}} + e^{\beta h_d^{(i,z)}}(1+e^{\beta g_u^{(i,z+1)}}). \quad \text{(A7)}$$

Finally, the free-energy shift due to a link addition between two side branches with root sites i and j at height z is

$$e^{-\beta\Delta F^{(i|j,z)}_{link,2}} = 1 + e^{\beta h_s^{(i,z)}} + e^{\beta h_s^{(j,z)}}. \quad \text{(A8)}$$

In order to compute the free energy of the system, we have to compute the mean values of the free-energy shifts for all the sites at a given height and for all the possible realization of the lattice. In the following, these mean values will be computed in three different cases: (1) A fluidlike homogeneous phase; (2) a crystallinelike solution characterized by the breakdown of the horizontal translational invariance; and (3) a glassy phase by a one-step replica symmetry breaking.

The fluidlike solution is obtained by setting the local fields on each layer the same for all sites of the layer ($\{\mathbf{h}^{(i,z)}\}=\{\mathbf{h}^{(z)}\}\forall i$). In this case, Eqs. (A4) become $5H-1$ algebraic coupled equations and they are easily solved finding the fixed points. This homogeneous (replica symmetric) solution is characterized by horizontal translational invariance and is found to be stable for high values of the configurational temperature, T_{conf}, or for low values of the number of grains per unit surface, N_s. In this case, the free energy is easily computed from Eqs. (A6), (A8), and (A7), since in this case all the quantities are site-independent. From the free energy F, we derive the density profile $\sigma(z)\equiv\langle n_i(z)\rangle$,

$$\sigma(z) = \frac{e^{\beta(\mu-mgz)}(1+e^{\beta g_u^{(z+1)}})}{e^{-\beta\Delta F^{(z)}_{site}}}, \quad \text{(A9)}$$

the number of particles per unity of surface, $N_s\equiv\Sigma_{z=1}^{H}\sigma(z)$, and the gravitational energy density $E\equiv\Sigma_{z=1}^{H}mgz\sigma(z)$. From the relation $F=E-TS-\mu N_s$, we also calculate the entropy per lattice site, $S=-\beta F-\beta\mu N_s+\beta E$.

In the crystalline (replica symmetric) solution, the local fields are different on different sites (breakdown of translational invariance), but do not fluctuate from site to site. This is achieved by introducing two sublattices, a and b, and different local fields on each lattice. The merging is done taking into account the structure of the crystalline phase. In our case, each site of the sublattice a (b) is connected with $k+1$ sites of the sublattice b (a). The crystal periodicity is thus two lattice spacings. Schematically, Eqs. (A4) for each layer become

$$\{\mathbf{h_a}\} = \mathbf{f}(\beta,\mu,\{\mathbf{h_b}\}),$$

$$\{\mathbf{h_b}\} = \mathbf{f}(\beta,\mu,\{\mathbf{h_a}\}),$$

where $\{\mathbf{h_a}\}$ and $\{\mathbf{h_b}\}$ are the sets of all local fields, respectively, on the two sublattices. This is a system of $2(5H-1)$ algebraic coupled equations. The free energy is computed from the fixed points of these equations. For a given N_s, by lowering T_{conf}, a phase transition from the fluid to the crystal is found at T_m (see Fig. 3).

The fluid phase still exists below T_m as a metastable phase corresponding to a supercooled fluid when crystallization is avoided. Nevertheless, the entropy per site predicted by the fluid solution becomes negative when the temperature is lowered. The fluid solution is definitely not appropriate to describe this region, and therefore we have to look for another kind of solution: A solution characterized by the presence of a large number of local minima of the free energy appears at a temperature T_D, and becomes stable at a temperature $T_K<T_D$, higher than the temperature where the entropy of the supercooled fluid becomes negative (see Fig. 13).

To describe this situation where the local fields may fluctuate, we have to introduce three probability distributions on each layer—$\mathcal{P}^{u}_{i,z}(h_u,g_u)$, $\mathcal{P}^{s}_{i,z}(h_s)$, and $\mathcal{P}^{d}_{i,z}(h_d,g_d)$—defined as the probability of finding the fields $h_u^{(i,z)}$ and $g_u^{(i,z)}$ (or, respectively, $h_s^{(i,z)}$ or $h_d^{(i,z)}$ and $g_d^{(i,z)}$) on site i at height z equal to h_u and g_u (or, respectively, to h_s or to h_d and g_d). Since the glassy phase is expected to be translational invariant, we work in the factorized case in which the probability distributions at a given height are equal for all the sites of the layer ($\mathcal{P}^{u,s,d}_{i,z}\equiv\mathcal{P}^{u,s,d}_{z}$).

The region at high packing fraction (or at low configurational temperature) is characterized by the existence of many metastable states, i.e., configurations which locally minimize the free energy. The number of such states for a given value of the free energy of the system is given by $\mathcal{N}(F)\sim\exp[N\Sigma(F)]$, where the function $\Sigma(F)$ is called complexity. Within the one-step replica symmetry breaking ansatz of the

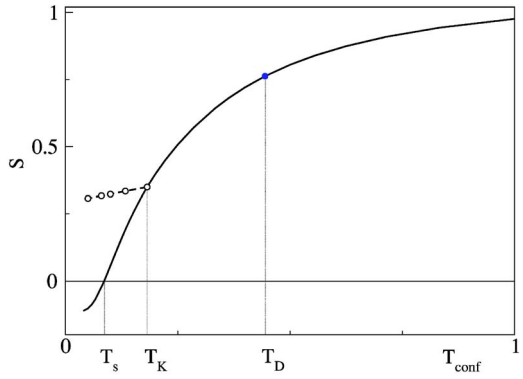

FIG. 13. Entropy density, S, as a function of the configurational temperature, T_{conf} (S is in units of K_B and T_{conf} in units of mga_0/K_B), in the liquid phase (RS solution) for $N_s=0.6$. A solution characterized by the presence of a large number of local minima of the free energy appears at a temperature T_D, and becomes stable at a temperature T_K.

cavity method (see Appendix B), the recursion relations for the fields are replaced by self-consistent integral equations for the probability distribution of the fields. For the "up" merging, the self-consistent integral equation reads

$$\mathcal{P}_z^u(h_u^z, g_u^z) = \mathcal{C}_1 \int \prod_{j=1}^{k-1} [dh_s^{(j,z)} \mathcal{P}_z^s(h_s^{(j,z)})] \times [dh_u^{(i,z+1)} dg_u^{(i,z+1)} \mathcal{P}_{z+1}^u(h_u^{(i,z+1)}, g_u^{(i,z+1)})] \times \delta(h_u^z - h_u^{(i,z)}) \delta(g_u^z - g_u^{(i,z)}) e^{-\beta m \Delta F_{up}^{(i,z)}}, \tag{A10}$$

where $\mathcal{C}_1$ is a constant insuring the normalization of $\mathcal{P}_z^u$, $h_u^{(i,z)}$ and $g_u^{(i,z)}$ are the local fields defined by Eqs. (A4), $m \in [0,1]$ is the usual 1RSB parameter to be obtained by the maximization of the free energy with respect to it, and ΔF_{up}^z is the free-energy shift in the "up" merging process. This quantity is computed by using the fact that the addition of a site i at a certain height z ("site addition") is the result of an "up" merging process, which creates a new "up" branch with root site i, plus a link addition between this branch and a down branch at height $z-1$,

$$\Delta F_{site}^{(i,z)} = \Delta F_{up}^{(i,z)} + \Delta F_{link,1}^{(i,z-1|z)}. \tag{A11}$$

From this equation, we obtain that

$$e^{-\beta \Delta F_{up}^{(i,z)}} = \frac{\bar{Z}_{0,u}^{(i,z)}}{\bar{Z}_{0,u}^{(i,z+1)} \prod_{j=1}^{k-1} Z_{0,s}^{(j,z)}}. \tag{A12}$$

From Eqs. (A1)–(A3), the free-energy shift $\Delta F_{up}^{(i,z)}$ has a simple expression in terms of the local fields.

In the same way, we can determine the self-consistency equations for the other two kinds of merging,

$$\mathcal{P}_z^s(h_s^z) = \mathcal{C}_2 \int \prod_{j=1}^{k-2} [dh_s^{(j,z)} \mathcal{P}_z^s(h_s^{(j,z)})] \times [dh_d^{(i,z-1)} dg_d^{(i,z-1)} \mathcal{P}_{z-1}^d(h_d^{(i,z-1)}, g_d^{(i,z-1)})] \times [dh_u^{(i,z+1)} dg_u^{(i,z+1)} \mathcal{P}_{z+1}^u(h_u^{(i,z+1)}, g_u^{(i,z+1)})] \times \delta(h_s^z - h_s^{(i,z)}) e^{-\beta m \Delta F_{side}^{(i,z)}} \tag{A13}$$

and

$$\mathcal{P}_z^d(h_d^z, g_d^z) = \mathcal{C}_3 \int \prod_{j=1}^{k-1} [dh_s^{(j,z)} \mathcal{P}_z^s(h_s^{(j,z)})] \times [dh_d^{(i,z-1)} dg_d^{(i,z-1)} \mathcal{P}_{z-1}^d(h_d^{(i,z-1)}, g_d^{(i,z-1)})] \times \delta(h_d^z - h_d^{(i,z)}) \delta(g_d^z - g_d^{(i,z)}) e^{-\beta m \Delta F_{down}^{(i,z)}}. \tag{A14}$$

For the "side" and the "down" merging, one has that

$$\Delta F_{site}^{(i,z)} = \Delta F_{side}^{(i,z)} + \Delta F_{link,2}^{(i|j,z)} \tag{A15}$$

and

$$\Delta F_{site}^{(i,z)} = \Delta F_{down}^{(i,z)} + \Delta F_{link,1}^{(i,z|z+1)}. \tag{A16}$$

This yields

$$e^{-\beta \Delta F_{side}^{(i,z)}} = \frac{Z_{0,s}^{(i,z)}}{\bar{Z}_{0,u}^{(i,z+1)} \bar{Z}_{0,d}^{(i,z-1)} \prod_{j=1}^{k-2} Z_{0,s}^{(j,z)}} \tag{A17}$$

and

$$e^{-\beta \Delta F_{down}^{(i,z)}} = \frac{\bar{Z}_{0,d}^{(i,z)}}{\bar{Z}_{0,d}^{(i,z+1)} \prod_{j=1}^{k-1} Z_{0,s}^{(j,z)}}. \tag{A18}$$

For any value of β, μ, and m, we solve Eqs. (A10), (A13), and (A14) iteratively, discretizing the probability distributions until the whole procedure converged.

From the probability distributions, we compute the free-energy density of the system: according to Eq. (A5), we have to find the average values of the free-energy shifts due to link and site additions. The free-energy shift due to site addition is given by

$$\langle e^{-\beta m \Delta F_{site}(z)} \rangle = \int \prod_{j=1}^{k-1} [dh_s^{(j,z)} \mathcal{P}_z^s(h_s^{(j,z)})] \times [dh_d^{(i,z-1)} dg_d^{(i,z-1)} \mathcal{P}_{z-1}^d(h_d^{(i,z-1)}, g_d^{(i,z-1)})] \times [dh_u^{(i,z+1)} dg_u^{(i,z+1)} \mathcal{P}_{z+1}^u(h_u^{(i,z+1)}, g_u^{(i,z+1)})] \times e^{-\beta m \Delta F_{site}(i,z)}. \tag{A19}$$

For the first kind of link addition, we have

$$\langle e^{-\beta m \Delta F^{(z)}_{link,1}} \rangle = \int [dh_d^{(i,z-1)} dg_d^{(i,z-1)} \mathcal{P}^d_{z-1}(h_d^{(i,z-1)}, g_d^{(i,z-1)})] \times [dh_u^{(i,z+1)} dg_u^{(i,z+1)} \mathcal{P}^u_{z+1}(h_u^{(i,z+1)}, g_u^{(i,z+1)})] \times e^{-\beta m \Delta F^{(i,z-1|z)}_{link,1}}. \quad \text{(A20)}$$

Finally, for the second kind of link addition, we find

$$\langle e^{-\beta m \Delta F^{(z)}_{link,2}} \rangle = \int \prod_{j=1}^{2} [dh_s^{(j,z)} \mathcal{P}^s_z(h_s^{(j,z)})] e^{-\beta m \Delta F^{(i|j,z)}_{link,2}}. \quad \text{(A21)}$$

In the previous relations, $\Delta F_{site}(i,z)$, $\Delta F^{(i,z-1|z)}_{link,1}$, and $\Delta F^{(i|j,z)}_{link,2}$ are functions of the local fields according to Eqs. (A6)–(A8).

The total free-energy density of the system is, according to Eq. (A5),

$$F[m] = -\frac{1}{\beta m}\left[\sum_{z=1}^{H} \log e^{-\beta m \Delta F^{(z)}_{site}} - \sum_{z=1}^{H} \frac{(k-1)}{2} \log e^{-\beta m \Delta F^{(z)}_{link,2}} - \sum_{z=1}^{H-1} \log e^{-\beta m \Delta F^{(z)}_{link,1}}\right]. \quad \text{(A22)}$$

The parameter m is fixed by the maximization of the free energy with respect to it. The justification for that is in the replica method, since m turns out to be the breakpoint in Parisi's order parameter function at the one-step RSB level. For a spin glass, it has been rigorously proved that in the limit $k \to \infty$, $F[m]$ is a lower bound to the correct free energy, so it is natural to find the preferred value of m by the maximization of $F[m]$.

From the knowledge of $F[m]$, it is indeed possible to compute the complexity $\Sigma(F)$ by Legendre transforming the function $F[m]$ itself [20],

$$\Sigma(F) = \beta m^2 \frac{\partial F[m]}{\partial m}. \quad \text{(A23)}$$

From this equation, we see that the maximization of $F[m]$ with respect to m corresponds exactly to the condition that the complexity vanishes. This relation also allows us to evaluate T_K.

First of all, for any given values of T_{conf} and μ, we solve numerically Eqs. (A10), (A13), and (A14) using an iterative procedure, for different values of the parameter m. This allows us to determine the field probability distributions. At this point, we can compute the function $F[m]$ via the relation expressed in Eq. (A22). For high configurational temperature (or low grain surface density), the iterative algorithm converges to the liquid solution, i.e., the field distribution functions turn out to be δ functions peaked around the fixed point of the liquid solution. As T_{conf} is decreased (or N_s is increased), a first nontrivial solution of the equations discontinuously appears at T_D for $m=1$. At this point, many states appear. However, the maximum of $F[m]$ with respect to m is found at $m>1$. Thus, such states are only metastable, the equilibrium state of the system being still given by the liquid. T_D is identified as a dynamical transition because at this point the equilibrium dynamics should display an ergodic-nonergodic transition due to the emergence of the metastable states. In this case, the complexity is found to be positive.

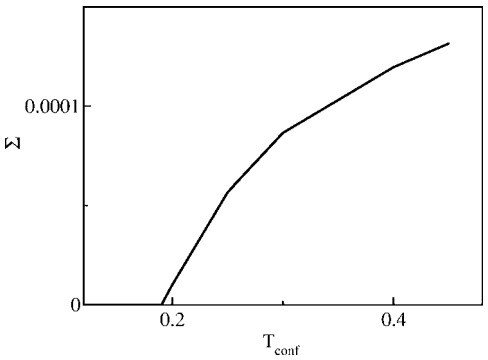

FIG. 14. Complexity, Σ, as a function of the configurational temperature, T_{conf} (Σ is in units of K_B and T_{conf} in units of mga_0/K_B), in the one-step RSB solution for $N_s=0.6$. At T_K, the complexity becomes zero.

The static transition appears at lower temperature, T_K, where the complexity vanishes (see Fig. 14). In order to obtain T_K, we can directly look for the temperature where $\partial_m F[m=1]=0$. For lower values of the configurational temperature ($T_{conf}<T_K$), the maximum of $F[m]$ with respect to m is found at $0<m<1$. The location of this maximum equals $m=1$ at $T_{conf}=T_K$ and tends to zero as $T_{conf}\to 0$. This is the same behavior found in p-spin models.

APPENDIX B: SELF-CONSISTENCY EQUATIONS IN THE CAVITY METHOD

In this appendix, we show how to obtain the self-consistency integral Eqs. (A10), (A13), and (A14) using the cavity method in the one-step RSB ansatz [11,12]. The region at high packing fraction (or at low configurational temperature) is characterized by the existence of many pure states. Let $\mathcal{N}(F)$ be the number of pure states for a given value of the free-energy density of the system. The function $N\Sigma(F)=\log \mathcal{N}(F)$ is called complexity. We assume that within one pure state α, the local fields $h^{(i,z)}_{u,\alpha}$, $g^{(i,z)}_{u,\alpha}$, $h^{(i,z)}_{s,\alpha}$, $h^{(i,z)}_{d,\alpha}$, and $g^{(i,z)}_{d,\alpha}$ on different cavity sites are uncorrelated. Therefore, Eqs. (A4) continue to hold in any given pure state. In this case, we have to make a statistical description of the solutions of Eqs. (A4) in the different pure states, taking into account the number of pure states for a given value of the free energy.

Let us consider, for example, the "up" merging of k cavity sites in a site i at height z. As said before, in each pure state α the local fields in the k cavity sites are not correlated. Nevertheless, in each pure state α the local fields, $(h^{(i,z)}_{u,\alpha}, g^{(i,z)}_{u,\alpha})$, and the free-energy shift, $\Delta F^{(i,z)}_{u,\alpha}$, due to the merging are correlated, since they are both functions of the local fields in the neighbor sites in the state α, according to Eqs. (A4) and (A11). Let us define $\mathcal{S}_z(h^z_u, g^z_u, \Delta F^z_u)$ as the probability distribution of finding the fields $(h^{(i,z)}_{u,\alpha}, g^{(i,z)}_{u,\alpha})$ and the free-energy shift ΔF^z_u after an up merging at height z. Because of the recursion relations of Eqs. (A4) and (A11), this distribution probability has to verify the following iteration relation:

$$\mathcal{S}_z(h_u^z, g_u^z, \Delta F_u^z) = \int \prod_{j=1}^{k-1} [dh_s^{(j,z)} \mathcal{P}_z^s(h_s^{(j,z)})][dh_u^{(i,z+1)} dg_u^{(i,z+1)} \times \mathcal{P}_{z+1}^u(h_u^{(i,z+1)}, g_u^{(i,z+1)})] \delta(h_u^z - h_u^{(i,z)}) \times \delta(g_u^z - g_u^{(i,z)}) \delta(\Delta F_u^z - \Delta F_u^{(i,z)}). \quad \text{(B1)}$$

In order to determine the probability distribution for the local fields self-consistently, we have to make the integration over all possible free-energy shifts,

$$\mathcal{P}_z^u(h_u^z, g_u^z) = \int d(\Delta F_u^z) \mathcal{S}_z(h_u^z, g_u^z, \Delta F_u^z) \mathcal{N}(F - \Delta F) = \int d(\Delta F_u^z) \mathcal{S}_z(h_u^z, g_u^z, \Delta F_u^z) e^{N\Sigma[(F-\Delta F_u^z)/N]}.$$

Since we are interested only in the local minima with the lowest free energies, we expand the exponent to the first order in ΔF_u^z,

$$\mathcal{P}_z^u(h_u^z, g_u^z) = \mathcal{C}_1 \int d(\Delta F_u^z) \mathcal{S}_z(h_u^z, g_u^z, \Delta F_u^z) \exp(-\beta m \Delta F_u^z), \quad \text{(B2)}$$

where the parameter $m \in [0,1]$ is

$$m = \frac{1}{\beta} \frac{\partial \Sigma}{\partial F}, \quad \text{(B3)}$$

and $\mathcal{C}_1$ is a normalization constant. Actually, the first-order expansion means that the density of pure states for a given value of the free energy is $\mathcal{N} \simeq \exp[m(F - F_{ref})]$, where F_{ref} is a reference free energy whose value is completely irrelevant. This form of the density of states is the same found in the one-step RSB formulation.

By integrating over ΔF_u^z, the δ function selects only the right value of the free-energy shift given in Eq. (A12). We thus have

$$\mathcal{P}_z^u(h_u^z, g_u^z) = \mathcal{C}_1 \int \prod_{j=1}^{k-1} [dh_s^{(j,z)} \mathcal{P}_z^s(h_s^{(j,z)})] \times [dh_u^{(i,z+1)} dg_u^{(i,z+1)} \mathcal{P}_{z+1}^u(h_u^{(i,z+1)}, g_u^{(i,z+1)})] \times \delta(h_u^z - h_u^{(i,z)}) \delta(g_u^z - g_u^{(i,z)}) e^{-\beta m \Delta F_u^z}. \quad \text{(B4)}$$

We have thus obtained the self-consistency Eq. (A10). In the same way, it is possible to obtain the equations for the "side" and the "down" merging.

[1] A. Coniglio and H. J. Herrmann, Physica A **225**, 1 (1996); M. Nicodemi, A. Coniglio, and H. J. Herrmann, Phys. Rev. E **55**, 3962 (1997).

[2] A. J. Liu and S. R. Nagel, Nature (London) **396**, 21 (1998).

[3] C. S. O'Hern, S. A. Langer, A. J. Liu, and S. R. Nagel, Phys. Rev. Lett. **86**, 111 (2001).

[4] G. D'Anna and G. Gremaud, Nature (London) **413**, 407 (2001); G. D'Anna, P. Mayor, A. Barrat, V. Loreto, and F. Nori, *ibid.* **424**, 909 (2003).

[5] A. Mehta and J. Berg, Europhys. Lett. **56**, 784 (2001).

[6] C. S. O'Hern, L. E. Silbert, A. J. Liu, and S. R. Nagel, Phys. Rev. E **68**, 011306 (2003).

[7] M. Nicodemi and A. Coniglio, Phys. Rev. Lett. **82**, 916 (1999).

[8] M. Nicodemi, Phys. Rev. Lett. **82**, 3734 (1999); A. Barrat, J. Kurchan, V. Loreto, and M. Sellitto, *ibid.* **85**, 5034 (2000); J. J. Brey, A. Prados, and B. Sánchez-Rey, Physica A **275**, 310 (2000); D. S. Dean and A. Lefèvre, Phys. Rev. Lett. **86**, 5639 (2001); H. A. Makse and J. Kurchan, Nature (London) **415**, 614 (2002); J. Berg, S. Franz, and M. Sellitto, Eur. Phys. J. B **26**, 349 (2002); G. De Smedt, C. Godreche, and J. M. Luck, Eur. Phys. J. B **32**, 215 (2003); G. Tarjus and P. Viot, Phys. Rev. E **69**, 011307 (2004).

[9] A. Coniglio and M. Nicodemi, Physica A **296**, 451 (2001); A. Fierro, M. Nicodemi, and A. Coniglio, Europhys. Lett. **59**, 642 (2002); **60**, 684 (2002); Phys. Rev. E **66**, 061301 (2002).

[10] S. F. Edwards and R. B. S. Oakeshott, Physica A **157**, 1080 (1989); A. Mehta and S. F. Edwards, *ibid.* **157**, 1091 (1989); S. F. Edwards, in *Current Trends in the Physics of Materials* (Italian Phys. Soc., North Holland, Amsterdam, 1990).

[11] M. Mézard and G. Parisi, Eur. Phys. J. B **20**, 217 (2001).

[12] G. Biroli and M. Mézard, Phys. Rev. Lett. **88**, 025501 (2002).

[13] M. PicaCiamarra, M. Tarzia, A. de Candia, and A. Coniglio, Phys. Rev. E **67**, 057105 (2003); **68**, 066111 (2003).

[14] L. F. Cugliandolo and J. Kurchan, Phys. Rev. Lett. **71**, 173 (1993); J. Kurchan, e-print cond-mat/9812347; and in *Jamming and Rheology*, edited by A. J. Liu and S. R. Nagel (Taylor and Francis, London, 2001).

[15] M. Tarzia, A. de Candia, A. Fierro, M. Nicodemi, and A. Coniglio, Europhys. Lett. **66**, 531 (2004).

[16] P. Philippe and D. Bideau, Europhys. Lett. **60**, 677 (2002).

[17] E. Clement and J. Rajchenbach, Europhys. Lett. **16**, 133 (1991).

[18] M. Tarzia, A. Fierro, M. Nicodemi, and A. Coniglio, Phys. Rev. Lett. **93**, 198002 (2004).

[19] In the case of uniform density profile, i.e., $\sigma(z)$=const, we have $\sigma(z)=\Phi$ [where $\Phi \equiv N/L^2(2\langle z \rangle - 1)$] below the maximum height and zero above.

[20] R. Monasson, Phys. Rev. Lett. **75**, 2847 (1995).

[21] C. Toninelli, G. Biroli, and D. S. Fisher, Phys. Rev. Lett. **92**, 185504 (2004).

[22] In the simulations at temperature, T_Γ, we choose randomly a particle and a nearest-neighbor cell: The particle is moved to the nearest-neighbor cell with a probability e^{-mg/T_Γ} if the final cell is up with respect to the initial one, and with a probability 1 if the final cell is down or on the same layer.

[23] J. B. Knight, C. G. Fandrich, C. N. Lau, H. M. Jaeger, and S. R. Nagel, Phys. Rev. E **51**, 3957 (1995); E. R. Nowak, J. B. Knight, E. Ben-Naim, H. M. Jaeger, and S. R. Nagel, *ibid.* **57**, 1971 (1998).

[24] We add a fully empty layer in $z=-1$ and a fully occupied layer in $z=0$ in order to simulate the box bottom, and a fully empty

layer in $z=L+1$ to allow the particles to occupy the top of the box without violating the hard-core interaction.

[25] W. Gotze, in *Liquids, Freezing and Glass Transition*, edited by J. P. Hansen, D. Levesque, and Zinn-Justin (Elsevier, Amsterdam, 1991); T. Franosch, M. Fuchs, W. Gotze, M. R. Mayr, and A. P. Singh, Phys. Rev. E **55**, 7153 (1997); M. Fuchs, W. Gotze, and M. R. Mayr, *ibid.* **58**, 3384 (1998).

[26] The β correlator predicted by the MCT is given by $\Phi(t)=f_c+g(t/t_\sigma)$, where $g(t/t_\sigma)\propto(t/t_\sigma)^{-a}$ for $t_0\ll t\ll t_\sigma$, and $g(t/t_\sigma)\propto -(t/t_\sigma)^b$ for $t_\sigma\ll t\ll\tau_\alpha$.

[27] We have verified that the relaxation time, τ, defined by $\langle q(\tau)\rangle\sim 0.1$, is proportional to the relaxation time obtained by fitting $\langle q(t)\rangle$, at very long time, with an exponential function. The advantage of the definition adopted here is to have smaller errors.

[28] J. A. Arenzon, Y. Levin, and M. Sellitto, Physica A **325**, 371 (2003).

[29] S. Franz, C. Donati, G. Parisi, and S. C. Glotzer, Philos. Mag. B **79**, 1827 (1999); C. Donati, S. Franz, S. C. Glotzer, and G. Parisi, J. Non-Cryst. Solids **307**, 215 (2002).

[30] N. Lačević, F. W. Starr, T. B. Schrøder, and S. C. Glotzer, J. Chem. Phys. **119**, 7372 (2003); S. C. Glotzer, V. N. Novikov, and T. B. Schrøder, *ibid.* **112**, 509 (2000).

[31] Interestingly, this anomalous behavior seems to occur around the crossover temperature T_D previously calculated. The origin of this behavior, also observed in molecular-dynamics simulations of a usual glass former [30], is still unclear.

[32] We add an auxiliary layer at height $H+1$ where all sites are empty in order to allow the particles to occupy the top of the box without violating the hard-core interaction. For the first two layers, $z=1,2$, we assume that the particles are always mechanically stable in order to simulate the presence of the bottom of the box.